New Materials, Compounds and Applications
Vol.6, No.3, 2022, pp.230-242

EFFECT OF Au DOPING ON ZnO NANOPARTICLES SENSITIVITY TO ETHANOL: A THERMODYNAMIC AND DENSITY FUNCTIONAL THEORY STUDY

Mudar Ahmed Abdulsattar[1,2*], Hayder M. Abduljalil[3], Hussein Hakim Abed[3]

[1]Department of Pharmacy, Al-Rasheed University College, Baghdad, Iraq
[2]Ministry of Science and Technology, Baghdad, Iraq
[3]Department of Physics, College of Science, University of Babylon, Iraq

Abstract. The effect of gold doping on zinc oxide nanoparticles' sensitivity to ethanol (C_2H_6O) and other gases is discussed using density functional theory. Bell–Evans–Polanyi principle is used to calculate the activation energy of the considered reactions. Gibbs free energy, enthalpy, and activation energy of the reacting gases with ZnO or Au/ZnO show that C_2H_6O has a higher reaction rate than the other calculated gases. Arrhenius equation parameters for one gas are used to calculate the reaction rate between all other gases and both pristine and Au-doped ZnO. Calculations included the effect of the ethanol burning with oxygen in the air before reaching the sensor surface. The highest reaction rate and optimum sensitivity temperature are between the flash point and autoignition temperatures of ethanol. The theory also shows that response time is inversely proportional to gas concentration, while recovery time is approximately linearly proportional to gas concentration.

Keywords: *Enthalpy energy, Au doping, ZnO cluster, ethanol, gas sensor, Gibbs free energy.*

Corresponding Author: *Mudar Ahmed Abdulsattar, Department of Pharmacy, Al-Rasheed University College, Baghdad, Iraq, e-mail: mudarahmed3@yahoo.com*

Received: *23 July 2022;* ***Accepted:*** *16 November 2022;* ***Published:*** *7 December 2022.*

1. Introduction

ZnO doping with Au is permanently used for numerous applications such as a gas sensor, optical modulation, piezoelectricity, water splitting (Wang *et al.*, 2022; Hoang *et al.*, 2022; Macková *et al.*, 2022; Chen *et al.*, 2022). ZnO alone or with other materials has been practically used for sensing many industrial or environmental gases such as C_2H_6O, CO, H_2, CH_4, CH_4O, NO, H_2S, H_2O (Eyvaraghi *et al.*, 2022; Kim *et al.*, 2018; Yahya *et al.*, 2019; Zhou *et al.*, 2022; Yu *et al.*, 2019). In many of these gases, the addition of noble metals, such as Pt, Au, Ag, Pd, etc., increases the sensitivity to the detected gas. ZnO molecules or particles at the nanoscale are called wurtzoids (Abdulsattar 2017; Abdulsattar, 2015). These molecules have been used frequently in gas sensing calculations (Abdulsattar 2017; Abdulsattar *et al.*, 2021).

Au is used as a gas sensor enhancer with many semiconductors, such as SnO_2 and Si (Guo *et al.*, 2022; Efeoğlu & Turut, 2022). The use of Au enhances the sensitivity and reduces response time appreciably. Au is added as a dopant or surface decoration or hybridization depending on the sensing material manufacturing method.

How to cite (APA):
Abdulsattar, M.A., Abduljalil, H.M., Abed H.H. (2022). Effect of Au doping on ZnO nanoparticles sensitivity to ethanol: a thermodynamic and density functional theory study. *New Materials, Compounds and Applications*, *6*(3), 230-242.

Ethanol is a material with a variety of uses that span medical, pharmaceutical, fuel, wine, industrial, etc. (Gundogan *et al.*, 2020; Liu *et al.*, 2022a; 2022b; Gonzalez *et al.*, 2021). As a result, the sensing of ethanol becomes of great importance. Ethanol sensors are made of a variety of materials; however, to gain high sensitivity and selectivity, certain sensors attracted wide attention with several experimental research to facilitate such applications.

Experimental results that illustrate the system of Au-doped ZnO and its sensitivity to ethanol are available (Eyvaraghi *et al.*, 2022; Zou *et al.*, 2019). Theoretical results about the upper-mentioned subject are less available (Eyvaraghi *et al.*, 2022). Since temperature is an important factor in gas sensing optimum conditions, thermodynamics are unavoidable in gas sensing, which was not addressed before. The present work addresses this deficiency.

In the present work, the Density functional theory is used to simulate the interaction of ethanol and other gases with ZnO and Au/ZnO. Evaluation of interaction energies such as Gibbs free energy, enthalpy, and activation energy between ethanol and sensing material is performed. Formulas for the response and recovery times that explain the trend of experimental data are given. Calculations included the effect of ethanol burning with oxygen in the air before reaching the sensor surface. Gibbs free energy and enthalpy are obtained without any experimental parametrization, while the activation energy is obtained from the limited experimental response time of one gas and applied to all the other gases. The limitation of available experimental results is the main obstacle to applying the present method.

2. Theory

The chemo-resistive sensors are discussed in the present work. The resistivity of the sensor material changes as it is exposed to the detected gas. The resistivity of the sensor is measured by a circuit that contains a heater to find the best working temperature of the sensor. The sensor material is exposed to the detected gas and normal air alternatively to register resistance changes.

All molecules in the present work are geometrically optimized using Gaussian 09 program (Frisch *et al.*, 2013) Dispersion corrections are added at the GD3BJ level because of the importance of this correction in gas sensing calculations (Rajput *et al.*, 2022). The B3LYP method in density functional theory has been used repeatedly with success for the simulation of ZnO molecules (Xu & Nezhad, 2022; Ahmed & Senthilkumar, 2022). The basis functions used in any ZnO molecular or nanoparticle calculations depend on the size of simulated molecules. 6-311G** basis functions are frequently used in ZnO calculations (Al-Rawi & Aljanabi, 2021; Fahmy *et al.*, 2021). B3LYP/6-311G** method and basis are found appropriate in ZnO wurtzoids calculations (Abdulsattar, 2017; Abdulsattar & Almaroof, 2017).

As we mentioned in the introduction, ZnO wurtzoids are used to represent ZnO particles at the nanoscale. The molecule (ZnO wurtzoid2c) is chosen for this purpose (Abdulsattar, 2015). Wurtzoids are the nearest molecules to ZnO nanoparticles having the wurtzite structure, as shown in Fig. 1(a). Adding a gold atom to ZnO wurtzoid2c also requires the addition of an oxygen atom to the molecule to gain stability, as in the equation:

$$Au/Zn_{13}O_{13}+½O_2 \rightarrow Au/Zn_{13}O_{14}\ (\Delta G=-0.87\ eV). \quad (1)$$

In the above equation ΔG is the change in Gibbs free energy of the reaction. When

the value of ΔG is negative, this means that the reaction will proceed in the forward direction. As we reach the $Au/Zn_{13}O_{14}$ molecule (Fig. 1b), adding or removing oxygen atoms from this molecule has a positive free energy which means that it is a stable molecule in an oxygen environment.

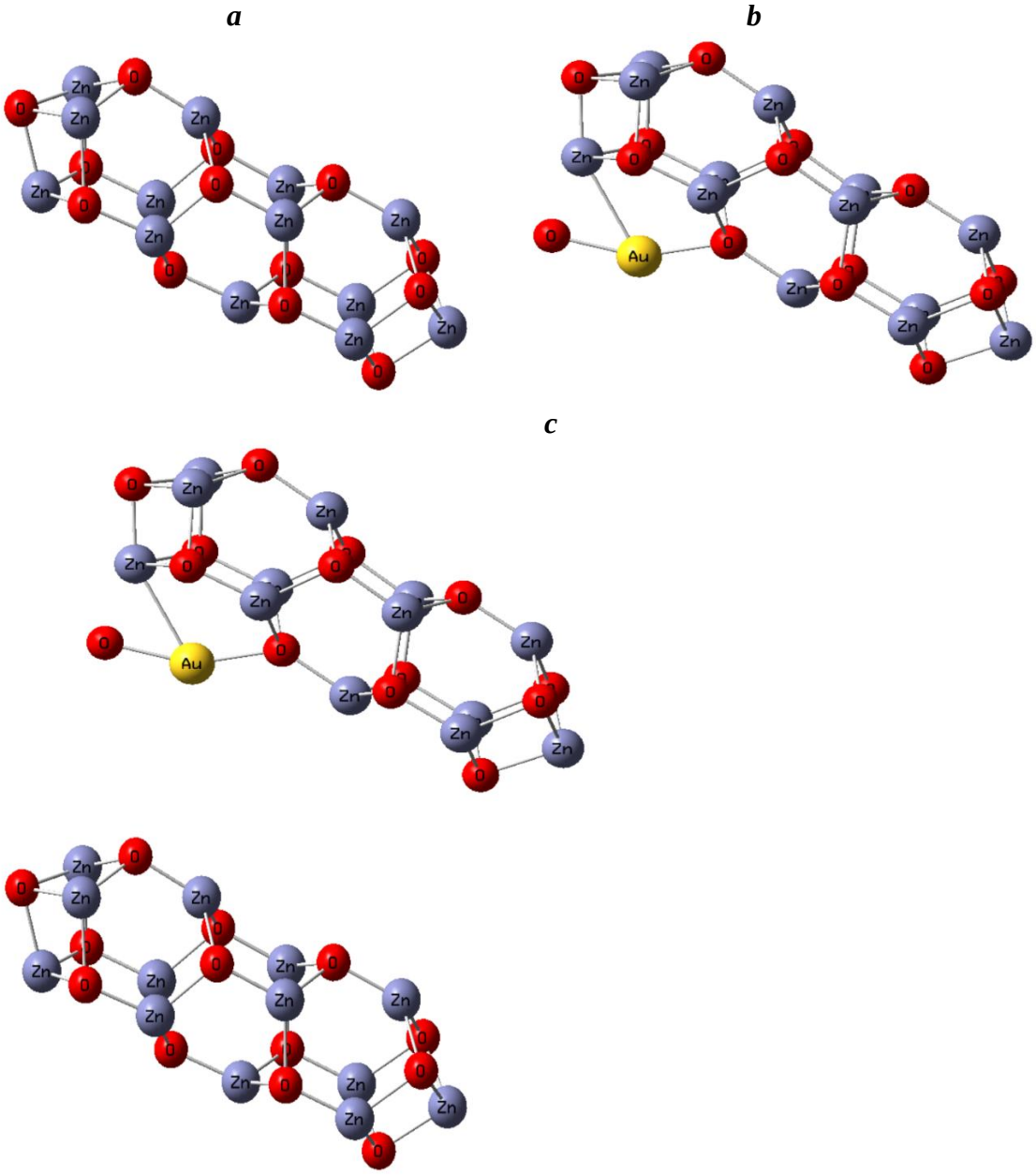

Fig. 1. (a) $Zn_{13}O_{13}$ cluster molecule (pristine ZnO), (b) $AuZn_{13}O_{14}$ cluster molecule with approximately 20% wt. Au (Au decorated ZnO), (c) two molecules $AuZn_{13}O_{14}$+ $Zn_{13}O_{13}$ (one pristine and one Au decorated ZnO) with approximately 10% wt. Au

The reaction of ethanol with oxygen in the air can be given by the reaction:

$$3O_2+C_2H_6O \rightarrow 3H_2O+2CO_2 \ (\Delta G=-12.284 \text{ eV}). \quad (2)$$

This reaction starts at 14℃ if the ignition is given by a suitable source. This temperature is called the flash point temperature (Do Nascimento *et al.*, 2021). At autoignition temperature, ethanol will ignite without the need for an external source in a

normal atmosphere. This temperature for ethanol is 450℃ (Li *et al.*, 2017). The reaction rate of ethanol in air in Eq. (2) can be given by:

$$\frac{d[C_2H_6O]}{dt} = -[O_2][C_2H_6O]k(T). \quad (3)$$

In the above equation, $[C_2H_6O]$ and $[O_2]$ are the concentration of ethanol and oxygen in the air, respectively. k(T) is the temperature-dependent part of the reaction rate that can be given by the Arrhenius equation:

$$k(T) = A\exp^{\left(\frac{-E_a}{k_B T}\right)}. \quad (4)$$

In the above equation, A is a preexponential constant, E_a is the activation energy, and k_B is the Boltzmann constant. The reaction of ethanol with the ZnO molecule in Fig. (1a) can be given by the equation:

$$6Zn_{13}O_{13}+C_2H_6O \rightarrow 6Zn_{13}O_{12}+3H_2O+2CO_2 \ (\Delta G=-5.364eV). \quad (5)$$

As we can see from the above equation that the Gibbs free energy of the reaction is negative so that the reaction will proceed forward. However, the absolute value of free energy of this reaction is much less than that in Eq. (2), so it is much slower than that in Eq. (2). The reaction rate of ethanol with ZnO molecules can be given by:

$$\frac{d[O]}{dt} = -[O][C_2H_6O]_e k(T). \quad (6)$$

In the above equation, [O] is the concentration of oxygen in ZnO molecules, $[C_2H_6O]_e$ is the effective concentration of ethanol near the surface of ZnO molecules due to the reaction of ethanol with oxygen in the air before it reaches the surface of the molecules as in Eq. (2). Solving Eq. (6), we have:

$$[O] = [O]_0 \exp^{-[C_2H_6O]_e k(T)t} \quad (7)$$

In the above equation, $[O]_0$ is the initial concentration of oxygen in ZnO molecules. From the above equation, we can determine the (response time) needed for the ethanol to reach 90% of its final value:

$$t_{res(90\%)} = \frac{\ln(10)}{[C_2H_6O]_e A\exp^{\left(\frac{-E_a}{k_B T}\right)}} = \frac{D}{[C_2H_6O]_e} \quad (8)$$

As we can see from the above equation that the response time is inversely proportional to the effective ethanol concentration. As suggested by Eq. (2), the use of effective concentration is not limited to ethanol but also applies to oxygen in the recovery phase. The effective concentration of oxygen near the ZnO molecule's surface is given by:

$$[O_2]_e = [O_2]_0 - \sigma[C_2H_6O] \quad (9)$$

Some of the oxygen in the air near the ZnO surface is replaced by the reaction product of Eq. (2), namely H_2O and CO_2, which are proportional to the reacting ethanol concentration as in Eq. (9). In the recovery phase, oxygen reacts with oxygen-deficient ZnO molecules ($Zn_{13}O_{12}$ in Eq. (5)) by the equation:

$$Zn_{13}O_{12}+½O_2 \rightarrow Zn_{13}O_{13} \ (\Delta G=-1.153 \text{ eV}). \quad (10)$$

Repeating the same steps of response time for the 90% recovery time we have:

$$t_{rec(90\%)} = \frac{\ln(10)}{[O_2]_e A \exp\left(\frac{-\Delta E_a}{k_B T}\right)} = \frac{E}{[O_2]_0 - \sigma[C_2H_6O]}. \quad (11)$$

3. Results and discussion

In Fig. (1a), the weight percentage of gold is 0%, while in Fig. 1(b), the weight percentage of gold is approximately 20% by weight. In Fig. 1(c), the weight percentage of gold is 10% by weight. In all three cases, a, b, or c, we must perform DFT calculations of $Zn_{13}O_{13}$, $AuZn_{13}O_{14}$, or both separately. Usually, van der Waals forces between nanoclusters (as in Fig. 1(c)) are too weak to change the structure of either cluster appreciably. The effect of increasing the weight percentage of gold can be handled by the Arrhenius equation parameters of Eq. (4), as we shall see shortly. The optimum weight percentage of Au in experiments can be anywhere between 0.5 to 15 wt% (Gu,*et al.*, 2021). The Arrhenius equation parameters of a certain structure can be applied to the reaction of all gases as predicted by Bell–Evans–Polanyi principle (Chen *et al.*, 2021).

Fig. (2) shows the Gibbs free energy of the reaction of several gases (C_2H_6O, CH_4O, CH_4, CO, H_2, NO, and H_2S) with both the ZnO molecule ($Zn_{13}O_{13}$) and the Au/ZnO molecule ($AuZn_{13}O_{14}$) at room temperature. Note that free energy and enthalpy values are obtained from DFT calculations without the use of experimental parameters. A negative value of Gibbs free energy of a reaction is an indicator that the reaction is spontaneous and is called an exergonic reaction. On the other hand, the positive value of Gibbs free energy of a reaction is an indicator that the reaction is nonspontaneous and is called an endergonic reaction. As we can see from Fig. (2), that the reactions with Au/ZnO are always more spontaneous than with ZnO alone. Ethanol reaction has the most negative values in both ZnO and Au/ZnO, followed by methanol and methane. H_2 and CO also have negative free energies and can be detected by ZnO or Au/ZnO. For NO gas, the free energy is positive in both ZnO and Au/ZnO. A weak sensitivity is driven by weak van der Waals forces or the reaction ($\alpha A + \beta B \rightarrow \rho R$) equilibrium constant as in the equation:

$$K_{eq} = \frac{[R]^{\rho}}{[A]^{\alpha}[B]^{\beta}} = e^{\frac{-\Delta G}{kT}} \quad (12)$$

As we can see from the above equation that positive values of free energy will produce a limited number of the reaction product [R] with respect to reactants [A] and [B]. To increase the sensitivity of ZnO or Au/ZnO to NO gas, we must either change the structure and the temperature or add another material. The same is true for H_2S gas in ZnO only.

The sensitivity to gas is affected by the enthalpy or the heat produced or absorbed in the reaction, as stated by Bell–Evans–Polanyi principle (Chen *et al.*, 2021):

$$E_a = E_0 + \alpha \Delta H. \quad (13)$$

In the above equation, E_a is the activation energy, ΔH is the enthalpy of the reaction, E_0 and α are parameters to be adjusted with other reaction data to obtain the activation energy. The enthalpy of reactions of gases with ZnO ($Zn_{13}O_{13}$) or Au/ZnO ($AuZn_{13}O_{14}$) is shown in Fig. 3. We can see from Fig. 3 that the same results that are obtained from Gibbs free energy of Fig. (2) apply to Fig. 3 for the enthalpy. We can use

the fitting parameters E_0=0.3 eV and α=0.05 (in Eq. (13)) to obtain the experimental response time of pristine ZnO or with 4 wt.% Au for the optimum operating conditions of reference (Eyvaraghi *et al.*, 2022). From these parameters, we can obtain Fig. (4) for the activation energy. Unlike Gibbs free energy and enthalpy, the lower the value of activation energy, the higher rate of reaction. The lowest activation energies are for C_2H_6O in its reactions with ZnO and Au/ZnO. The highest activation energies are for NO and H_2S, which are the same gases with positive or small negative values of free energy and enthalpy.

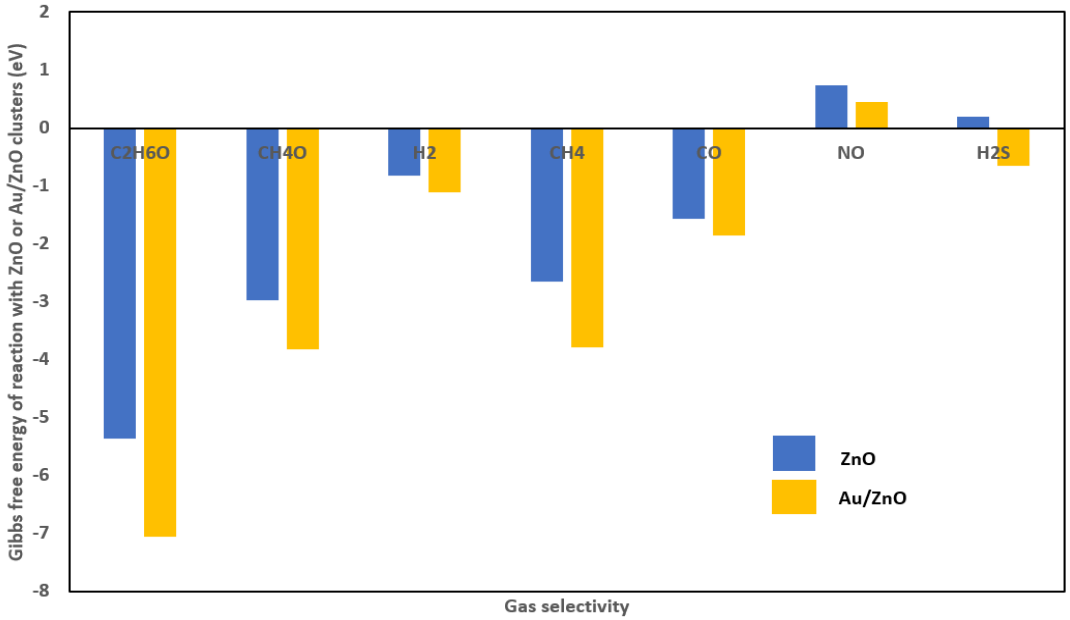

Fig 2. Gibbs free energy of reaction of several gases (C_2H_6O, CH_4O, CH_4, CO, H_2, NO, and H_2S) with both ZnO molecule ($Zn_{13}O_{13}$ in Fig 1(a)) and the Au/ZnO molecules ($AuZn_{13}O_{14}$ in Fig 1(b))

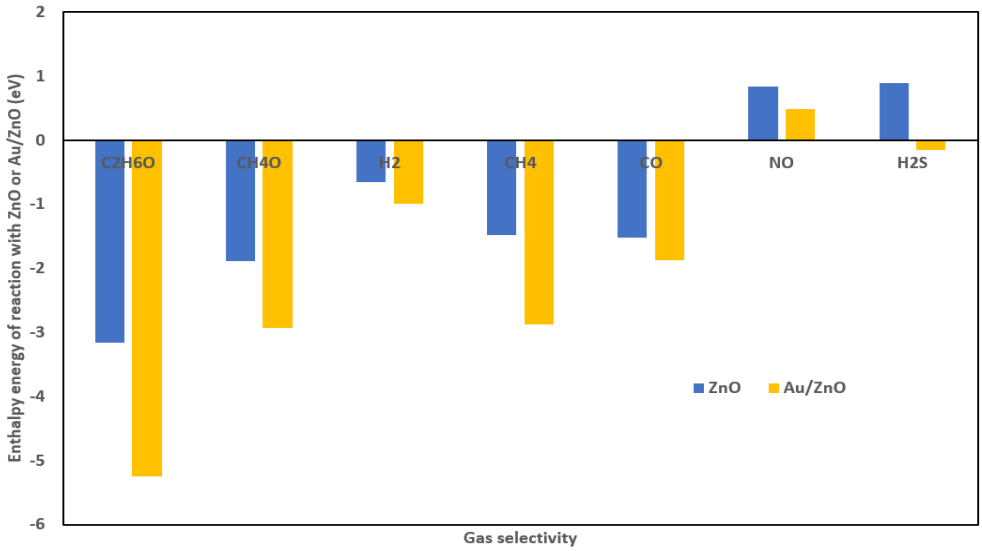

Fig 3. Enthalpy of reaction of several gases (C_2H_6O, CH_4O, CH_4, CO, H_2, NO, and H_2S) with both ZnO molecule ($Zn_{13}O_{13}$ in Fig 1(a)) and the Au/ZnO molecules ($AuZn_{13}O_{14}$ in Fig 1(b))

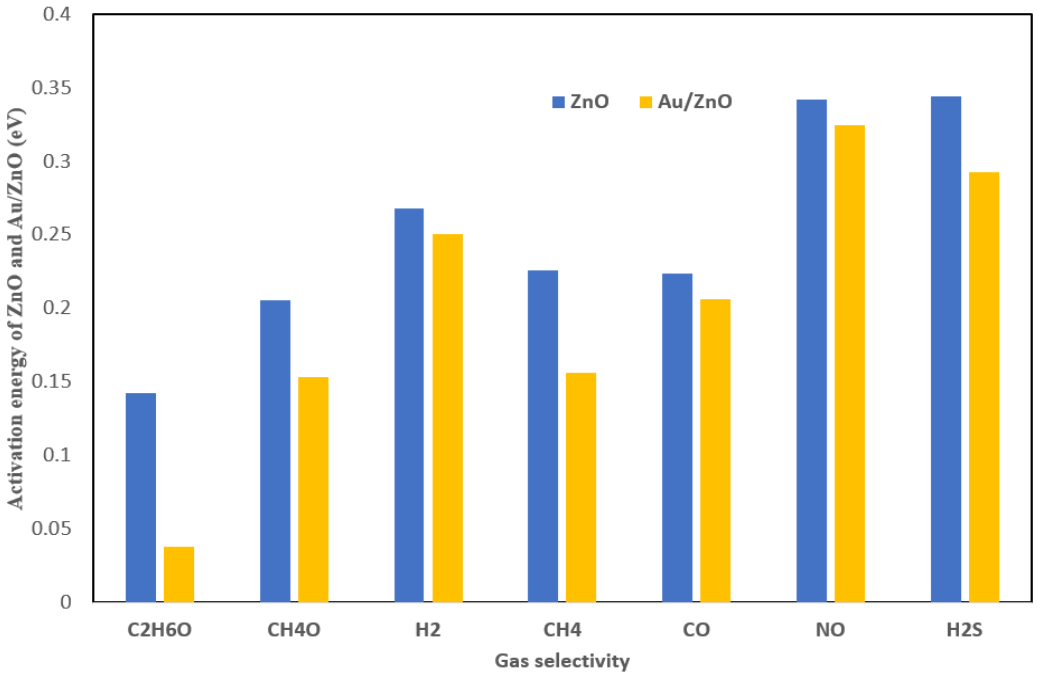

Fig 4. Activation energy of reaction of several gases (C_2H_6O, CH_4O, CH_4, CO, H_2, NO, and H_2S) with both pristine ZnO molecule and the Au 4% wt./ZnO molecules. Eq. (13) is used to evaluate the activation energy

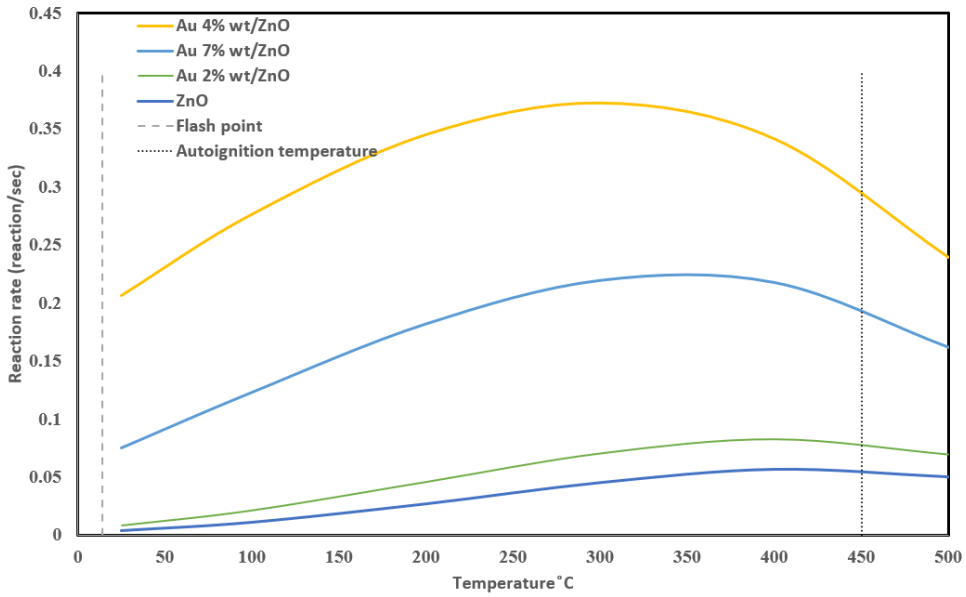

Fig 5. Theoretical reaction rate of C_2H_6O with both ZnO molecules and the Au/ZnO molecules (Au 2, 4, 7 wt.%). Flash point and autoignition temperature of ethanol are shown

Fig. 5 shows the reaction rate of ethanol with both ZnO and Au/ZnO with various Au weight content. Flash point (Do Nascimento *et al.*, 2021) and autoignition temperatures (Li *et al.*, 2017) of ethanol are shown. For ZnO, Fig. (5) is obtained by solving two Arrhenius equations for the reactions in Eq. (2) and (5). The same is performed for Au/ZnO. The preexponential factor and activation energy of Eq. (2), (5),

and other needed reactions are all given in Table 1 for ZnO and Au/ZnO. A quantity of ethanol is burnt in the air before it reaches ZnO or Au/ZnO surface. Ethanol burning in the air is the dominant reaction in both ZnO and Au/ZnO when they reach autoignition temperature. Logically, the temperature with the highest reaction rate with ZnO or Au/ZnO is the temperature with the highest sensitivity. This temperature in Fig. (5) is approximately 400 and 300℃ for ZnO and Au 4% wt./ZnO, respectively. The Au 2 and 7% weight only differ by activation energy (0.12 and 0.0639 eV, respectively) and not a preexponential factor. Experimental highest sensitivity temperature values range between 225 to 450℃ for ZnO and Au/ZnO (do Nascimento *et al.,* 2021; Zhang *et al.,* 2016; Kang *et al.,* 2021). Both references (Zhang *et al.,* 2016; Kang *et al.,* 2021) agree with our calculations that Au/ZnO highest sensitivity temperature is lower than that of ZnO.

Fig. (6) Shows the response time as a function of ethanol concentration for ZnO and Au 4% wt./ZnO. Unfortunately, the experimental data in reference (Eyvaraghi *et al.,* 2022) only gives values at the optimized operating temperature of 400℃ and for ethanol concentration 100 ppm. However, other references such as reference (Subha & Jayaraj, 2019) gives the same trend in our calculations but for ZnO and CuO/ZnO. Our theoretical results are based on Eq. (8).

Fig. (7) shows the recovery time as a function of ethanol concentration for ZnO and Au 4% wt./ZnO. Experimental values are from reference (Zou *et al.,* 2016). Our theoretical results are based on Eq. (11). The same trend can be found for ZnO and CuO/ZnO in reference (Subha & Jayaraj, 2019).

Fig. (8) shows the reaction rates of ZnO, Au 2, 4, and 7% wt./ZnO as a function of ethanol concentration at 400℃. As we mentioned above, the reaction rate represents the resistivity or response of the sensor to a specific concentration of ethanol. The linear relation of reaction rate to concentration can be seen in Eq. (6). The present results are in agreement with the results of references (Eyvaraghi *et al.,* 2022; Zou *et al.,* 2016; Subha & Jayaraj, 2019).

Table 1. Arrhenius equations parameters fitted to response and recovery times of ZnO and Au 4% wt

No.	Reaction	A (s^{-1})	E_a (eV)	σ
1	$3O_2+C_2H_6O \rightarrow 3H_2O+2CO_2$	48	0.3000	-
2	$6Zn_{13}O_{13}+C_2H_6O \rightarrow 6Zn_{13}O_{12}+3H_2O+2CO_2$	9000	0.1421	-
3	$6Au/Zn_{13}O_{14}+C_2H_6O \rightarrow 6\ Au/Zn_{13}O_{13}+3H_2O+2CO_2$	9000	0.0378	-
4	$Zn_{13}O_{12}+½O_2 \rightarrow Zn_{13}O_{13}$	5000	0.2267	1400
5	$Au/Zn_{13}O_{13}+½O_2 \rightarrow Au/Zn_{13}O_{14}$	30000	0.2441	1000

The gas sensing mechanism is mainly affected by the surface structure and surface reconstruction more than the bulk lattice structure. As a result, nanoparticles usually are more effective in detecting gases than larger particles because of their higher surface area. The effect of surface area and lattice structure is considered by the (A) parameter in Eq. (4) in the Arrhenius equation. The unit of this parameter (as can be seen from Table 1 is s^{-1}, which represents the frequency of collisions of the detected gas with the sensor surface. For different crystalline surfaces or amorphous sensor surfaces, the differences lie in the area available for collisions between the gas and surface. For well-prepared surfaces, the number of collisions is high enough to increase the reaction rate

and sensitivity ((Eq. (3) and Eq. (4)) and reduce the response time (Eq. (8)) and/or recovery time (Eq. (11)). For poorly prepared surfaces the value of (A) is relatively low with lower sensitivity and higher response and recovery times. This parameter is fitted to the experimental results as in Table 1. The value of the (A) parameter can be a measure of the quality of the sensor surface for different structures or surfaces.

Many sensor mechanisms depend on the adsorption and desorption of the gas on the sensor surface without reactions. However, the reaction of the gas with the sensor material (if possible, with a negative Gibbs free energy) gives a higher sensor response since the reaction transforms the sensor (which is usually a metal oxide) gradually to metal by censored gas reaction as in Eq. (5) by reducing the metal oxide to metal. The formed oxygen-deficient metal oxide has a resistance that is lower relative to the oxygen-saturated metal oxide. The Gibbs free energy of adsorption is in the order of 1 eV or less compared to the 5.3 eV for reaction energy as in Eq. (5). Obviously, the activation energy of a reaction is much less than the adsorption energy as in Eq. (13), and hence higher response is obtained by reaction than that of adsorption. Also, some gases discussed in the present work, such as methane, are used to reduce ZnO to pure Zn (Chuayboon & Abanades, 2022), which proves the reaction of these gases with ZnO is unavoidable.

There is no doubt that the use of a larger number of atoms can give more correct results than using a small cluster of atoms (such as the cluster $Zn_{13}O_{13}$ in the present work). However, computational difficulties hamper the use of such a high number of atoms. As a result, the use of a logical number of atoms is very desired in such calculations. The interaction of gas molecules is mainly at the sensor surface. The interaction potential of the gas molecules decreases with the inverse distance between the gas molecule and the distant atoms in the sensor.

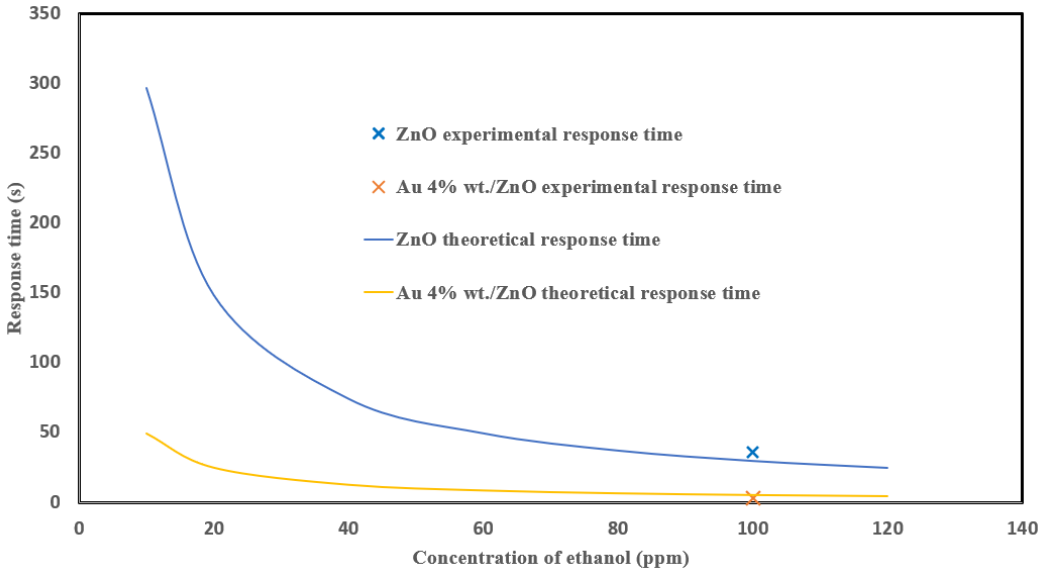

Fig. 6. Response time as a function of ethanol concentration at 400℃ for ZnO and Au/ZnO (4 wt.% Au). Experimental values are from reference Eyvaraghi *et al.*, (2022)

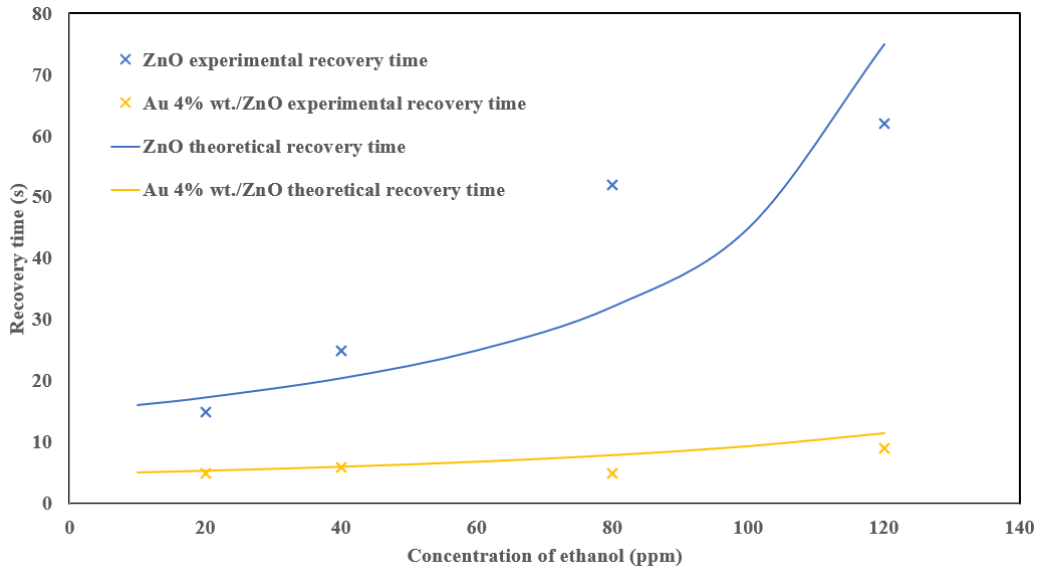

Fig. 7. Recovery time as a function of ethanol concentration at room temperature for ZnO and Au/ZnO. Experimental values are from reference Zou *et al.* (2016)

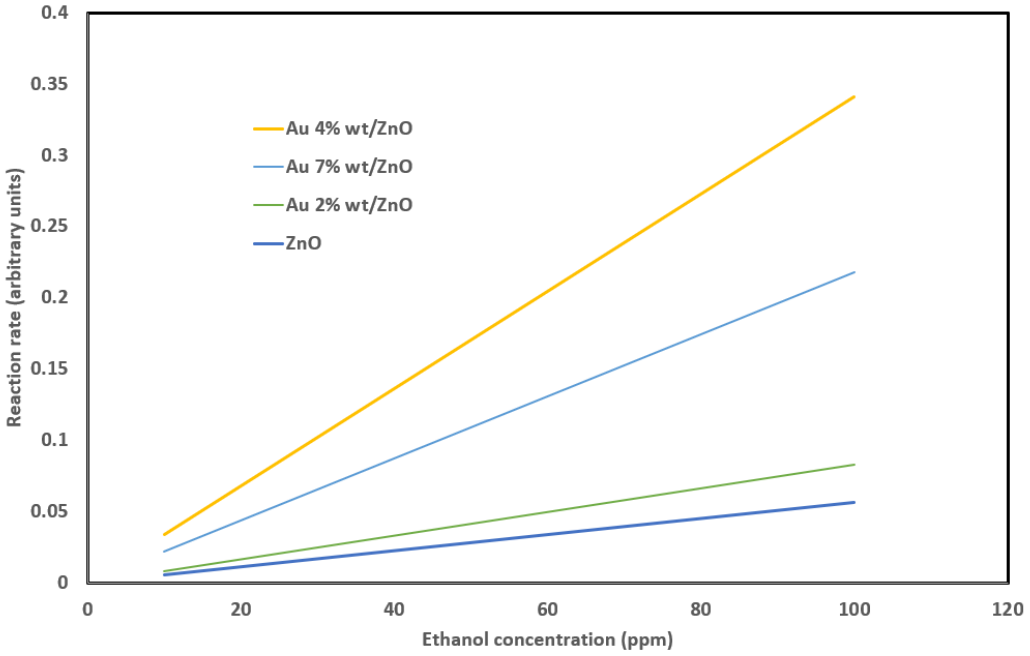

Fig. 8. Reaction rates of ZnO, Au 2, 4, and 7% wt./ZnO as a function of ethanol concentration at 400 ℃

In semiconductors, an additional exponentially damping factor exists due to charge movement. The long-range effects are suppressed by the flow of particles in response to electric fields. This flow reduces the effective interaction between particles to a short-range (screened Coulomb interaction). Practically, this shows that the use of even 2nd neighbors interaction is enough to obtain acceptable results. However, the use of 4th neighbors is more common in computational semiconductor physics (Abdulsattar & Al-Bayati, 2007; Abdulsattar, 2009). The present work uses more neighbors beyond the 4th neighborhood atoms.

4. Conclusions

Density functional theory can give good simulation to many trends in gas sensing problems, as proven by the present work. Gibbs free energy (or enthalpy) of reaction can be used to certify that the gas reactions are spontaneous or nonspontaneous (exothermic or endothermic). The enthalpy of the reaction can be used to determine the activation energy of these reactions using the Bell–Evans–Polanyi principle. Applying this method to the sensitivity of ZnO and Au/ZnO toward ethanol gas, we can find that ethanol gas has good selectivity over many gases such as CH_4O, CH_4, CO, H_2, NO, and H_2S. Using Arrhenius equations, the highest sensitivity and reaction rate is found near the experimental results in the range of 300 to 400℃ for the ethanol gas. Response time is found to be inversely proportional to gas concentration, while recovery time is linearly proportional to the gas concentration. Calculations included the effect of an ethanol burning with oxygen in the air before reaching the sensor surface. Results also show that the highest sensitivity temperature is located between flash point and autoignition temperatures. Theoretical results are in good agreement with available experimental results.

References

Abdulsattar, M.A. (2009). Size effects of semiempirical large unit cell method in comparison with nanoclusters properties of diamond-structured covalent semiconductors. *Physica E: Low-dimensional Systems and Nanostructures, 41*(9), 1679-1688.

Abdulsattar, M.A. (2015). Capped ZnO (3, 0) nanotubes as building blocks of bare and H passivated wurtzite ZnO nanocrystals. *Superlattices and Microstructures*, 85, 813-819.

Abdulsattar, M.A. (2017). Chlorine gas reaction with ZnO wurtzoid nanocrystals as a function of temperature: a DFT study. *Journal of Molecular Modeling, 23*(4), 1-6.

Abdulsattar, M.A., Al-Bayati, K.H. (2007). Corrections and parametrization of semiempirical large unit cell method for covalent semiconductors. *Physical Review B, 75*(24), 245201.

Abdulsattar, M.A., Almaroof, H.M. (2017). Adsorption of H_2 and O_2 gases on ZnO wurtzoid nanocrystals: A DFT study. *Surface Review and Letters, 24*(Supp01), 1850008.

Abdulsattar, M.A., Jabbar, R.H., Abed, H.H., & Abduljalil, H.M. (2021). The sensitivity of pristine and Pt doped ZnO nanoclusters to NH3 gas: A transition state theory study. *Optik*, 242, 167158.

Ahmed, E., Senthilkumar, K. (2022). First-principle investigation of defect-associated LVM and structural parameter dependency in response to the ground state on-site Hubbard correction of w-ZnO. *Journal of Raman Spectroscopy, 53*(6), 1166-1178

Al-Rawi, B.K., Aljanabi, S.M. (2021). Modeling the Physical Properties of ZnO Nanoparticles with Selective Hydrogen Using DFT. *International Journal of Nanoscience, 20*(01), 2150011.

Chen, Y., Chang, K.H., Meng, F.Y., Tseng, S.M., & Chou, P.T. (2021). Broadening the Horizon of the Bell–Evans–Polanyi Principle towards Optically Triggered Structure Planarization. *Angewandte Chemie, 133*(13), 7281-7288.

Chen, Y., Li, Y., Feng, B., Wu, Y., Zhu, Y., & Wei, J. (2022). Self-templated synthesis of mesoporous Au-ZnO nanospheres for seafood freshness detection. *Sensors and Actuators B: Chemical*, 360, 131662.

Chuayboon, S., Abanades, S. (2022). Thermochemical performance assessment of solar continuous methane-driven ZnO reduction for co-production of pure zinc and hydrogen-rich syngas. *Chemical Engineering Journal*, 429, 132356.

Do Nascimento, D.C., Conti, D.C., Neto, A.M.B., & Costa, M.C. (2021). Flash point measurement and prediction of dodecane+ ethanol+ FAEE systems. *Fuel*, 306, 121723.

Efeoğlu, H., Turut, A. (2022). A highly stable temperature sensor based on Au/Cu/n-Si Schottky barrier diodes dependent on the inner metal thickness. *Journal of Physics D: Applied Physics*, *55*(18), 185303.

Eyvaraghi, A.M., Mohammadi, E., Manavizadeh, N., Nadimi, E., Ma'mani, L., Broumand, F. A., & Zeidabadi, M.A. (2022). Experimental and density functional theory computational studies on highly sensitive ethanol gas sensor based on Au-decorated ZnO nanoparticles. Thin Solid Films, 741, 139014.

Fahmy, A., Khafagy, R.M., Elhaes, H., & Ibrahim, M.A. (2021). ICMMS-2: Molecular Modeling Analyses of Polyvinyl Alcohol/Sodium Alginate/ZnO Composite. *Egyptian Journal of Chemistry*, *64*(3), 1149-1166.

Frisch, M.J., Trucks, G.W., Schlegel, H.B., Scuseria, G.E., Robb, M.A., Cheeseman, J.R., ... & Nakai, H. (2013). Gaussian 09 citation. Gaussian Inc.: Wallingford.

Gonzalez, R., Guindal, A.M., Tronchoni, J., & Morales, P. (2021). Biotechnological Approaches to Lowering the Ethanol Yield during Wine Fermentation. *Biomolecules*, *11*(11), 1569.

Gu, F., Wang, Y., Han, D., & Wang, Z. (2021). Effects of ZnO crystal facet on the ethanol detection by the Au/ZnO sensors. *Talanta Open*, 4, 100068.

Gundogan, K., Dave, N.J., Griffith, D. P., Zhao, V.M., McNally, T.A., Easley, K.A., ... & Ziegler, T.R. (2020). Ethanol Lock Therapy Markedly Reduces Catheter-Related Blood Stream Infections in Adults Requiring Home Parenteral Nutrition: A Retrospective Study From a Tertiary Medical Center. *Journal of Parenteral and Enteral Nutrition*, *44*(4), 661-667.

Guo, L., Shen, Z., Ma, C., Ma, C., Wang, J., & Yuan, T. (2022). Gas sensor based on MOFs-derived Au-loaded SnO2 nanosheets for enhanced acetone detection. *Journal of Alloys and Compounds*, 906, 164375.

Hoang, Q.T., Ravichandran, V., Cao, T.G.N., Kang, J.H., Ko, Y.T., Lee, T.I., & Shim, M.S. (2022). Piezoelectric Au-decorated ZnO nanorods: ultrasound-triggered generation of ROS for piezocatalytic cancer therapy. *Chemical Engineering Journal*, 435, 135039.

Kang, Y., Zhang, L., Wang, W., & Yu, F. (2021). Ethanol sensing properties and first principles study of Au supported on mesoporous ZnO derived from metal organic framework ZIF-8. *Sensors*, *21*(13), 4352.

Kim, J. H., Mirzaei, A., Kim, H. W., & Kim, S. S. (2018). Low power-consumption CO gas sensors based on Au-functionalized SnO_2-ZnO core-shell nanowires. *Sensors and Actuators B: Chemical*, 267, 597-607.

Li, R., Liu, Z., Han, Y., Tan, M., Xu, Y., Tian, J., ... & Li, Z. (2017). Experimental and numerical investigation into the effect of fuel type and fuel/air molar concentration on autoignition temperature of n-heptane, methanol, ethanol, and butanol. *Energy & Fuels*, *31*(3), 2572-2584.

Liu, L., Liu, M., Zhang, Y., Feng, Y., Wu, L., Zhang, L., ... & Su, X. (2022a). The role of hydroxyl group of ethanol in the self-assembly of pharmaceutical cocrystal of myricetin with 4, 4′-bipyridine. *Journal of Molecular Structure*, 1250, 131848.

Liu, Z., Wei, D., Ji, M., Fang, H., & Zhou, H. (2022b). Combustion instability of ethanol and n-heptane fuels under different combustor geometries. *Journal of the Energy Institute*, 102, 206-215.

Macková, A., Malinský, P., Jagerová, A., Mikšová, R., Lalik, O., Nekvindová, P., ... & Galeckas, A. (2022). Energetic Au ion beam implantation of ZnO nanopillars for optical response modulation. *Journal of Physics D: Applied Physics*, *55*(21), 215101.

Rajput, K., He, J., Frauenheim, T., & Roy, D. R. (2022). Monolayer PC3: A promising material for environmentally toxic nitrogen-containing multi gases. *Journal of Hazardous Materials*, 422, 126761.

Subha, P.P., Jayaraj, M.K. (2019). Enhanced room temperature gas sensing properties of low temperature solution processed ZnO/CuO heterojunction. *BMC Chemistry*, *13*(1), 1-11.

Wang, S., Liu, P., Meng, C., Wang, Y., Zhang, L., Pan, L., ... & Zou, J.J. (2022). Boosting photoelectrochemical water splitting by Au@ Pt modified ZnO/CdS with synergy of Au-S bonds and surface plasmon resonance. *Journal of Catalysis*, 408, 196-205.

Xu, N.Y., Nezhad, P.D.K. (2022). Computational survey on the Pt-decorated ZnO nanosheet as a chemical sensor for chlorobenzene: Explaining the experimental observations. *Journal of Physics and Chemistry of Solids*, 161, 110379.

Yahya, N.A.M., Hamid, M.R.Y., Ong, B.H., Rahman, N.A., Mahdi, M.A., & Yaacob, M.H. (2019). H 2 gas sensor based on Pd/ZnO nanostructures deposited on tapered optical fiber. *IEEE Sensors Journal*, *20*(6), 2982-2990.

Yu, S., Zhang, H., Chen, C., & Lin, C. (2019). Investigation of humidity sensor based on Au modified ZnO nanosheets via hydrothermal method and first principle. *Sensors and Actuators B: Chemical*, 287, 526-534.

Zhang, H., Wu, S., Liu, J., Cai, Y., & Liang, C. (2016). Laser irradiation-induced Au–ZnO nanospheres with enhanced sensitivity and stability for ethanol sensing. *Physical Chemistry Chemical Physics*, *18*(32), 22503-22508.

Zhou, Q., Xu, L., Kan, Z., Yang, L., Chang, Z., Dong, B., ... & Song, H. (2022). A multi-platform sensor for selective and sensitive H_2S monitoring: Three-dimensional macroporous ZnO encapsulated by MOFs with small Pt nanoparticles. *Journal of Hazardous Materials*, 426, 128075.

Zou, A. L., Qiu, Y., Yu, J. J., Yin, B., Cao, G.Y., Zhang, H.Q., & Hu, L.Z. (2016). Ethanol sensing with Au-modified ZnO microwires. *Sensors and Actuators B: Chemical*, 227, 65-72.